Homogeneous Electron Transfer Catalysis of the Electrochemical Reduction of Carbon Dioxide. Do Aromatic Anion Radicals React in an Outer-Sphere Manner?

Armando Gennaro,[1a] Abdirisak A. Isse,[1a] Jean-Michel Savéant,*[,1b] Maria-Gabriella Severin,[1a] and Elio Vianello*[,1a]

Contribution from the Dipartimento di Chimica Fisica, Università di Padova, Via Loredan 2, 35131 Padova, Italy, and Laboratoire d'Electrochimie Moléculaire de l'Université Denis Diderot (Paris 7), 2 place Jussieu, 75251 Paris Cedex 05, France

Received February 26, 1996. Revised Manuscript Received April 17, 1996[⊗]

Abstract: Electrochemically generated anion radicals of aromatic nitriles and esters possess the remarkable property to reduce carbon dioxide to oxalate with negligible formation of carboxylated products. They may thus serve as selective homogeneous catalysts for the reduction of CO_2 in an aprotic medium. The catalytic enhancement of the cyclic voltammetric peaks of these catalysts is used to determine the rate constant of the electron transfer from these aromatic anion radicals to CO_2 as a function of the catalyst standard potential. Substituted benzoic esters allowed a particularly detailed investigation of the resulting activation-driving force relationship. Using 14 different catalysts in this series made it possible to finely scan a range of reaction standard free energies of 0.4 eV. Detailed analysis of the resulting data leads to the conclusion that the reaction is not a simple outer-sphere electron transfer. It rather consists in a nucleophilic addition of the anion radical on CO_2, forming an oxygen (or nitrogen for the nitriles)−carbon bond, which successively breaks homolytically, generating the parent ester (or nitrile) and the anion radical of CO_2, which eventually dimerizes to oxalate.

The continuous attention the chemistry of carbon dioxide attracts derives mostly from its abundance on earth as a carbon source and from the central role it plays in life processes. At the same time, the chemistry of CO_2 raises fundamental issues related to its single electron and electron pair acceptor properties, whatever the probabilities of its practical use as a cheap carbon source in the near future. Direct electrochemical reductive activation of CO_2 runs into the difficulty that a very negative potential (beyond −2.2 V vs SCE in an aprotic medium) is required. This fact has been an incentive for many attempts to catalyze the electrochemical reduction of CO_2. Molecules of particular interest in this respect are reduced states of transition metal complexes where electron transfer to CO_2 and the ensuing chemical steps are anticipated to take place within the metal coordination sphere.[2−4]

Anion radicals of unsaturated organic compounds, generated electrochemically in aprotic media, are expected to be single electron donors. They have been reacted with several acceptors such as alkyl halides, aryl alkyl sulfides,[5] and also CO_2. In a number of cases, the reaction with CO_2 does not give rise to catalysis but rather leads to carboxylation of the electron donor, a reaction that may be of synthetic interest.[2a] Monocarboxylates and/or dicarboxylates have thus been obtained from activated olefins[6] and polycyclic aromatic hydrocarbons.[7] N-heteroaromatic molecules similarly yield the corresponding dihydrocarboxy derivatives[8] while α-hydroxy and α-amino acids are produced from carbonyl compounds[9] and imines, respectively.[10] In these reactions, CO_2 has been considered to react with the anion radical either as an electron pair acceptor or as a single electron acceptor.

[⊗] Abstract published in *Advance ACS Abstracts,* July 1, 1996.

(1) (a) Università di Padova. (b) Université Denis Diderot.

(2) (a) For reviews see refs 2b and 2c and also the introduction of refs 3b−d. (b) Silvestri, G. In *Carbon Dioxide as a Source of Carbon*; Aresta, M., Forti, G., Eds.; NATO ASI Series C; Reidel: Dordrecht, 1987; p 339. (c) Collin, J. P.; Sauvage, J. P. *Coord. Chem. Rev.* **1989**, *93*, 245.

(3) (a) Hammouche, M.; Lexa, D.; Savéant, J.-M.; Momenteau, M. *J. Electroanal.* **1988**, 249, 347. (b) Hammouche, M.; Lexa, D.; Momenteau, M.; Savéant, J.-M. *J. Am. Chem. Soc.* **1991**, *113*, 8455. (c) Bhugun, I.; Lexa, D.; Savéant, J.-M. *J. Am. Chem. Soc.* **1994**, *116*, 5015. (d) Bhugun, I.; Lexa, D.; Savéant, J.-M. *J. Am. Chem. Soc.*, in press.

(4) (a) The transition metal CO_2 reduction catalysts that have received the most active attention are Ni and Co cyclams, rhenium carbonyl, and rhodium, iridium, osmium, and ruthenium bipyridine complexes (see the introduction of refs 3b−d) as well as cobalt(I) salen complexes.[4b,c] Iron(0) porphyrins are particularly efficient catalysts when combined with Brönsted or Lewis acid synergists.[3] (b) Gennaro, A.; Isse, A. A.; Vianello, E.; Floriani, C. *J. Mol. Catal.* **1991**, *70*, 197. (c) Gennaro, A.; Isse, A. A.; Vianello, E. in *Electrochemitstry of Inorganic, Bioinorganic and Organometallic Compounds,* Pombeiro, A. J. L., McCleverty, J. A., Eds.; Kluwer: Amsterdam, 1993; p 311.

(5) (a) For alkyl halides see refs 5b and 5c c and references therein. For aryl alkyl sulfides see ref 5d and references therein. (b) Savéant, J.-M. Single Electron Transfer and Nucleophilic Substitution. In *Advances in Physical Organic Chemistry;* Bethel, D., Ed.; Academic Press: New York, 1990; Vol. 26, pp 1−130. (c) Bertran, J.; Gallardo, I.; Moreno, M.; Savéant, J.-M. Submitted for publication. (d) Severin, M. G.; Arevalo, M. C.; Maran, F.; Vianello, E. *J. Phys. Chem.* **1993**, *97*, 150.

(6) (a) Tyssee, D. A.; Wagenknecht, J. H.; Baizer, M. M.; Chruma, J. L. *Tetrahedron Lett.* **1972**, *47*, 4809. (b) Tyssee, D. A.; Baizer, M. M. *J. Org. Chem.* **1974**, *39*, 2819. (c) Lamy, E.; Nadjo, L.; Savéant, J.-M. *Nouv. J. Chim.* **1979**, *3*, 21. (d) Gambino, S.; Filardo, G.; Silvestri, G. *J. Appl. Electrochem.* **1982**, *12*, 549. (e) Gambino, S.; Gennaro, A.; Filardo, G.; Silvestri, G.; Vianello, E. *J. Electrochem. Soc.* **1987**, *134*, 2172.

(7) (a) Wawzonek, S.; Wearing, D. *J. Am. Chem. Soc.* **1959**, *81*, 2067. (b) Ticianelli, E. A.; Avaca, L. A.; Gonzalez, E. R. *J. Electroanal. Chem.* **1989**, *258*, 369. (c) Ticianelli, E. A.; Avaca, L. A.; Gonzalez, E. R. *J. Electroanal. Chem.* **1989**, *258*, 379.

(8) (a) Hess, U.; Fuchs, P.; Jacob, E.; Lund, H. *Z. Chem.* **1980**, *20*, 64. (b) Fuchs, P.; Hess, U.; Holst, H. H.; Lund, H. *Acta Chem. Scand., Ser. B* **1981**, *35*, 185.

(9) (a) Wawzonek, S.; Gunderson, A. *J. Electrochem. Soc.* **1960**, *107*, 537. (b) Harada, J.; Y. Sakakibara, Y.; Kunai, A.; Sasaki, K. *Bull. Chem. Soc. Jpn.* **1984**, *57*, 611. (c) Ikeda Y.; Manda, E. *Bull. Chem. Soc. Jpn.* **1985**, *58*, 1723. (d) Silvestri, G.; Gambino, S.; Filardo, G. *Tetrahedron Lett.* **1986**, *27*, 3429. (e) Bulhoes L. O. D. S.; Zara, A. J. *J. Electroanal. Chem.* **1988**, *248*, 159. (f) Mcharek, S.; Heintz, M.; Troupel, M.; Perichon, J. *Bull. Soc. Chim. Fr.* **1989**, 95. (g) Chan, A. S. C.; Huang, T. T.; Wagenknecht, J. H.; Miller, R. E. J. *Org. Chem.* **1995**, *60*, 742.

(10) (a) Hess, U.; Thiele, R. *J. Prakt. Chem.* **1982**, *324*, 385. (b) Silvestri, G.; Gambino, S.; Filardo, G. *Gazz. Chim. Ital.* **1988**, *118*, 643.

S0002-7863(96)00605-1 CCC: $12.00

$$A^{\bullet -} + CO_2 \rightleftharpoons ACO_2^{\bullet -}$$

$$A^{\bullet -} + CO_2 \rightleftharpoons A + CO_2^{\bullet -}$$

In the former case, the carboxylated anion radical thus formed is further reduced to the dianion which is then protonated or carboxylated a second time:

$$ACO_2^{\bullet -} + e^- \text{ (and/or } A^{\bullet -}) \rightleftharpoons ACO_2^{2-} (+A)$$

$$ACO_2^{2-} + CO_2 (H^+) \rightarrow A(CO_2)_2^{2-} (AHCO_2^-)$$

In the second case, ACO_2^{2-} would be formed by coupling between the two anion radicals

$$CO_2^{\bullet -} + A^{\bullet -} \rightleftharpoons ACO_2^{2-}$$

before undergoing a second carboxylation or protonation as in the preceding case. Whatever its exact mechanism, mono- and dicarboxylation reactions correspond to a stoichiometry of two electrons per A molecule.

Carboxylation of A is not necessarily the only result of the reaction of the anion radicals of unsaturated organic compounds with CO_2. In several instances, the enhancement of the one-electron wave for the generation of the anion radical upon addition of CO_2 has been observed to overpass a 2e/molecule stoichiometry. In such cases, the current response takes a catalytic character, implying that products stemming from CO_2 alone, such as oxalate, formate, CO (+ carbonate), are formed instead of (or in addition to) carboxylation products. Such catalytic currents have been observed with chrysene,[7b,11a] picene,[7b] and benzonitrile.[11b] However, with the exception of benzonitrile where the formation of oxalate has been observed,[11b] CO_2 self-derived products have not been investigated.

The photochemistry of aromatic molecules in the presence of CO_2 has also been investigated as another means of triggering electron transfer. Photocarboxylation of several aromatic hydrocarbons, in the presence of various amines used as sacrificial electron donors, have thus been described.[12] Photocatalysis has been reported to occur to a small extent with anthracene, phenanthrene, and pyrene, and more efficiently with oligo(*p*-phenylenes), containing two−five monomer units, where formate is the main reaction product (the proton necessary for the formation of the C−H bond presumably comes from the oxidation of the sacrificial electron donor, usually an amine).[13]

We have found that substituted benzonitriles as well as a large variety of substituted and unsubstituted alkyl or phenyl benzoates catalyze the electrochemical reduction of CO_2 in *N*,*N*-dimethylformamide (DMF) with exclusive formation of oxalate. Under such circumstances, the analysis of the kinetics of electron transfer forming the $CO_2^{\bullet -}$ anion radical is greatly simplified. The use of an extended series (of 14 members) of benzoates then allowed a detailed investigation of the dynamics of the reaction. Whether electron transfer between these anion radicals and CO_2 is of the outer-sphere type or involves more intimate chemical interactions is a question that we will address on the basis of the experimentally established activation−driving force relationship.

(11) (a) Lund, H.; Simonet, J. *J. Electroanal. Chem.* **1975**, *55*, 205. (b) Filardo, G.; Gambino, S.; Silvestri, G.; Gennaro, A.; Vianello, E. *J. Electroanal. Chem.* **1984**, *177*, 303.

(12) (a) Tazuke, S.; Ozawa, H. *J. Chem. Soc., Chem. Commun*. **1975**, *237*. (b) Tazuke, S.; S. Kazama, S.; Kitamura, N. *J. Org. Chem.* **1986**, *51*, 4548. (c) Ito, Y.; Uozu, Y.; Matsuura, T. *J. Chem. Soc., Chem. Commun.* **1988**, 562.

(13) (a) Matsuoka, S.; Kohzuki, T.; Pac, C.; Ishida, A.; Takamuku, S.; Kusaba, M.; Nakashima, N.; Yanagida, S. *J. Phys. Chem.* **1992**, *96*, 4437. (b) Matsuoka, S.; Kohzuki, T. Pac, C.; Yanagida, S. *Chem. Lett.* **1990**, 2047.

Table 1. Homogeneous Catalysts: Designation, Standard Potentials, and Rate Constants of the Reaction with CO_2[a]

catalyst	designation	E°_{cat} (V vs SCE)	log k (M^{-1} s^{-1})
dimethyl phthalate	**1E**	-1.92_8	0.5_0
diisobutyl phthalate	**2E**	-1.94_8	0.8_2
dibutyl phthalate	**3E**	-1.95_8	0.9_0
methyl 4-phenylbenzoate	**4E**	-1.96_2	1.0_6
phenyl benzoate	**5E**	-2.02_6	2.1_5
phenyl 3-methylbenzoate	**6E**	-2.03_6	2.4_6
ethyl 3-fluorobenzoate	**7E**	-2.04_3	2.4_3
methyl 3-phenoxybenzoate	**8E**	-2.08_5	3.0_1
phenyl 4-methylbenzoate	**9E**	-2.09_4	3.0_8
methyl benzoate	**10E**	-2.20_2	4.1_9
ethyl benzoate	**11E**	-2.22_1	4.2_1
methyl 3-methylbenzoate	**12E**	-2.23_7	4.4_4
methyl 2-methylbenzoate	**13E**	-2.27_6	4.7_4
methyl 4-methylbenzoate	**14E**	-2.29_0	5.0_4
4-cyanobiphenyl	**1N**	-1.95_7	1.2_4
benzonitrile	**2N**	-2.26_0	5.3_1
2-tolunitrile	**3N**	-2.29_7	5.6_0

[a] In DMF + 0.1 M *n*-Bu_4NClO_4. Temperature 25 °C.

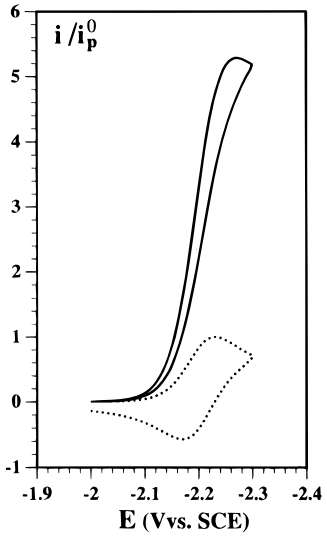

Figure 1. Cyclic voltammetry of **10E** (2.6 mM) in DMF + 0.1 M n-Bu_4NClO_4 in the absence (dotted line) and presence (solid line) of CO_2 (26 mM). The current scale is normalized toward the cathodic peak current in the absence of CO_2, i_p°. Scan rate 1 V/s. Temperature 25 °C.

Results

The various ester and nitrile catalysts that we have investigated are listed in Table 1 together with the conventional designations that will be used throughout the paper. In the absence of CO_2, these compounds all give rise to a reversible cyclic voltammetric wave. The standard potentials, E°_{cat}, that can be obtained from the midpoint between the cathodic and anodic peaks are important parameters for the following discussion. Their values, referenced to the aqueous SCE, are listed in Table 1.

Figure 1 shows a typical example of the reversible wave obtained with one of the ester catalysts, **10E**, and of the catalytic current observed upon addition of CO_2. Catalysis results in a loss of reversibility and an enhancement of the cathodic peak current.

Constant current electrolyses were carried out with several of these catalysts in the presence of CO_2 at potentials where

Table 2. Preparative Scale Electrolysis of CO_2 Catalyzed by Aromatic Ester and Nitrile Anion Radicals[a]

catalyst	$E°_{cat}$[e] (V vs SCE)	[cat] (mM)	[CO_2] (mM)	faradaic yields: oxalate	faradaic yields: CO
none			152	0.67_2	0.25_3
none[b]			102	0.41_9	0.48_3
5E	−2.026	1.14	114	0.79_0	0.00_1
10E	−2.202	1.63	101	0.84_0	0.00_1
10E[b]	−2.202	1.53	51	0.96_9	0.00_1
10E[b]	−2.202	1.54	102	0.93_7	0.00_5
10E[b]	−2.202	1.47	152	0.93_0	0.00_8
10E[b]	−2.202	1.39	262	0.99_7	0.00_3
10E[c]	−2.202	1.33	102	0.92_8	0.00_4
10E[d]	−2.202	1.54	102	0.90_2	0.00_9
2N	−2.260	1.84	101	0.74_0	0.00_1
2N	−2.260	2.10	21	0.80_0	0.00_7

[a] In DMF + 0.1 M *n*-Bu_4NClO_4 at a mercury pool electrode. Current density 1.6 mA/cm^2. Temperature is 25 °C unless otherwise stated. [b] Temperature 0 °C. [c] Temperature 10 °C. [d] Temperature −10 °C. [e] At 25 °C.

Scheme 1

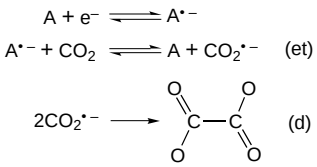

only the catalytic reduction takes place (the effective reduction potential was found to be slightly more positive than the standard potential of the catalyst). The results are displayed in Table 2. Analysis of products showed that oxalate is practically the only product formed whatever the temperature and the concentrations of catalyst and CO_2. Cyclic voltammetric examination of the solution after electrolysis revealed that the consumption of the catalyst after 30 turnovers is small, less than 30% (see the Experimental Section).

These results suggest the mechanism shown in Scheme 1. The CO_2 anion radicals formed from the ester or nitrile anion radicals in the et step undergo a fast dimerization (d) to oxalate. The formation of a carbon−oxygen adduct between $CO_2^{\bullet-}$ and CO_2 (ad) should however be envisaged in view of the Lewis

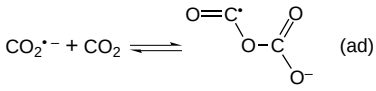

acid properties of CO_2 and the basic properties of $CO_2^{\bullet-}$. This intermediate has been previously invoked[14d−f] to explain the competitive formation of oxalate and CO in direct electrochemical reduction at inert electrodes such as mercury and lead.[14] Formation of CO and of an equimolar amount of carbonate was deemed to occur through reduction of this carbon−oxygen adduct.[14d−f] While this reaction may take place at the electrode surface, its counterpart in the solution (r), where the electron

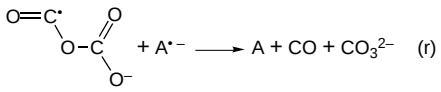

donor would be $A^{\bullet-}$ seems unable to compete with dimerization over the whole temperature range explored (Table 2) since practically no CO is found among the electrolysis products even when the CO_2 concentration is much higher than the steady-state concentration of $CO_2^{\bullet-}$, thus favoring the occurrence of reaction ad. The competition between steps ad + r and step d may be described quantitatively by the dimensionless parameter $K_{ad}k_r k_d^{-1/2}k^{-3/4}[CO_2]^{1/4}(I/FD^{1/2})^{1/2}$ (I is the current density and D the diffusion coefficient of CO_2).[15a] This should be less than 10^{-2} for the yield of CO to be smaller than 1%.[15a] In the results displayed in Table 2, the most favorable conditions for CO production involve catalyst **5E**. The experimental conditions (Table 2 and the Experimental Section) were such that $I/FD^{1/2} = 219$ M^{-1} dm^3 s$^{1/2}$; $k = 1.4 \times 10^2$ M^{-1} s^{-1} (Table 1). k_d can be estimated as 5×10^8 M^{-1} s^{-1} from previous high scan rate cyclic voltammetric experiments on the direct reduction of CO_2 in DMF at a mercury electrode.[15b,c] Thus, $K_{ad}\,k_r \le 10^3$ s^{-1}. A rough estimate of k_r can be derived from earlier electron photoinjection experiments in acetonitrile.[16a] The reduction potential of the CO_2−$CO_2^{\bullet-}$ adduct thereof appears to be *ca.* 240 mV positive of the reduction potential of CO_2,[16b,c] implying that k_r is roughly 2 orders of magnitude larger than k. Reaction ad would thus be slightly uphill ($K_{ad} \le 0.07$ M^{-1}).

The kinetics of reaction et may be derived from the relative enhancement of the peak current of the catalyst triggered by the addition of CO_2 to the solution, $i_p/i_p°$ as exemplified in Figure 1. Figure 2 summarizes, in a typical case, the procedure that we followed for measuring the rate constant k of reaction et. The theoretical variations of $i_p/i_p°$ were computed as a function of the rate dimensionless parameter $(RT/F)(k/\upsilon)$ by a finite difference method for the mechanism depicted in Scheme 1 where the et step was regarded as rate determining.[17] For given values of the catalyst concentration [cat] and of the ratio [CO_2]/[Cat], the parameter $(RT/F)(k/\upsilon)$ was varied by changing the scan rate. The value of k was determined from the best fitting of the data points with the theoretical curve. For each catalyst, several sets of such experiments were carried out with different values of [cat] and of the ratio [CO_2]/[cat] as illustrated in Figure 2. The experimental values of $i_p i_p°$ and the curve-fitting procedure are given in the supporting information for the whole series of ester (14) and nitrile (3) anion radicals. The resulting average values of log k (±0.1) are listed in Table 1.

The rate constant k diminishes as the standard potential of the catalyst becomes less and less negative as a consequence of the attending increase of the standard free energy of the reaction. A parallel increase of the reverse et reaction is expected. It is thus conceivable that, on going to less and less

(14) (a) Kaiser, U.; Heitz, E. *Ber. Bunsen-Ges. Phys. Chem.* **1973**, *77*, 818. (b) Gressin, J. C.; Michelet, D.; Nadjo, L.; Savéant, J.-M. *Nouv. J. Chim.* **1979**, *3*, 545. (c) Fisher, J.; Lehmann, T.; Heitz, E. *J. Appl. Electrochem.* **1981**, *11*, 743. (d) Amatore, C.; Savéant, J.-M. *J. Am. Chem. Soc.* **1981**, *103*, 5021. (e) Amatore, C.; Savéant, J.-M. *J. Electroanal. Chem.* **1981**, *125*, 22. (f) Amatore, C.; Nadjo, L.; Savéant, J.-M. *Nouv. J. Chim.* **1984**, *8*, 565.

(15) (a) Isse, A. A.; Savéant, J.-M.; Severin, M. G. *J. Electroanal. Chem.* **1995**, *399*, 157. (b) In the original publication[15c] a rough estimate of 10^7 M^{-1} s^{-1} was given. A more accurate simulation of the cyclic voltammograms, taking account of the large double layer charging current and of the fact than the scan is reverted not far from the foot of the cathode, gives a value of 5×10^8 M^{-1} s^{-1}. (c) Lamy, E.; Nadjo, L.; Savéant, J.-M. *J. Electroanal. Chem.* **1977**, *78*, 403.

(16) (a) Vassiliev, Y. B.; Bagotsky, V. S.; Khasova, O. A.; Mayorova, N. A. *J. Electroanal. Chem. Interfacial Electrochem.* **1985**, *189*, 295. (b) This estimation of the standard potential may seem at variance with an assumption often made in molecular electrochemistry, namely, that a radical deriving from the association of the primary anion radical with a Lewis or Brönsted acid is much easier to reduce than the starting molecule. The reduction rate constant should then be close to the diffusion limit. In fact, it may well be that the secondary radical is only moderately easier to reduce than the starting molecule or even harder to reduce. A striking example of the latter case is provided by the reduction of benzaldehyde in ethanolic media where it has been shown that the protonated anion radical is more difficult to reduce than benzaldehyde.[16c] (c) Andrieux, C. P.; Grzeszczuk, M.; Savéant, J.-M. *J. Am. Chem. Soc.* **1991**, *113*, 8811.

(17) (a) Andrieux, C. P.; Savéant, J.-M. Electrochemical Reactions. In *Investigations of Rates and Mechanisms;* Bernasconi, C. F., Ed.; Wiley: New York, 1986; Vol. 6, 4/E, Part 2, p 305. (b) Andrieux, C. P.; Hapiot, P.; Savéant, J.-M. *Chem. Rev.* **1990**, *90*, 723.

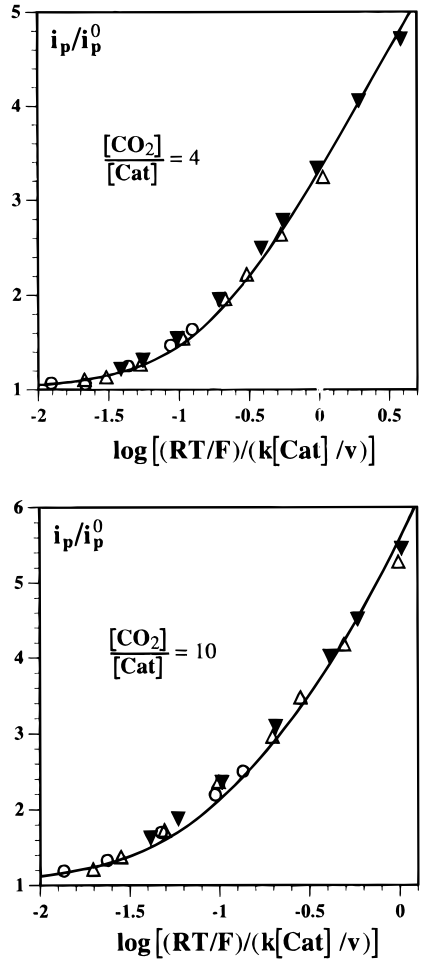

Figure 2. Cyclic voltammetry of **10E** in DMF + 0.1 M *n*-Bu_4NClO_4. Determination of the rate constant, *k*, of reaction et from the ratio of the peak currents in the presence (*i*p) and absence ($i_p°$) of CO_2. Temperature 25 °C. The solid lines are the theoretical curves with a value of *k* corresponding to the best fitting. The experimental conditions corresponding to the data points are as defined below:

$[CO_2]/[cat]$	data pts	[cat] (mM)	scan rate (V/s)
4	○	1.27	50, 35, 20, 10, 5, 3.5
	△	2.60	50, 35, 20, 10, 5, 3.5, 2, 1
	▼	4.62	50, 35, 20, 10, 5, 3.5, 2, 1, 0.5
10	○	1.27	50, 35, 20, 10, 5, 3.5
	△	2.60	50, 35, 20, 10, 5, 3.5, 2, 1
	▼	4.62	50, 35, 20, 10, 5, 3.5, 2

negative values of the standard potential of the catalyst, the kinetics pass from control by forward reaction et to partial control by reaction d. More precisely, the passage from the former situation to the latter is governed by the increase of the dimensionless parameter $K^2(k_d/k)$ where *k* is the forward rate constant for the et step, *K* its equilibrium constant $(RT/F) \ln K = E°_{CO_2-} E°_{cat}$ and k_d the dimerization rate constant. Simulation of the theoretical $i_p/i_p°$ variations showed that when the dimensionless parameter is smaller than 0.025, the interference of the dimerization in the kinetics ceases to be negligible. Under these conditions, the fitting of the data points was found to be less satisfactory than it is in the case where forward et is regarded as the rate-determining step. The fact that the forward et reaction is the rate-determining step implies that the overall dimerization rate constant is equal to or larger than 3×10^8 M^{-1} s^{-1}. This condition is fulfilled since $k_d = 5 \times 10^8$ M^{-1} s^{-1} as discussed earlier.

(18) Ovenall, D. W.; Whiffen, D. H. *Mol. Phys.* **1961**, 4, 135.

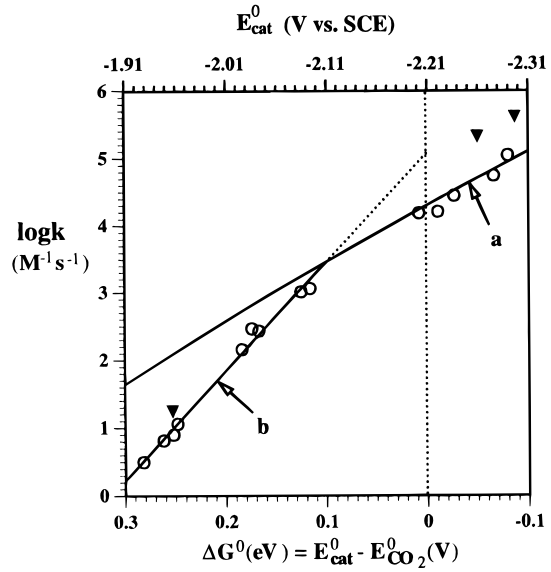

Figure 3. Variation of the rate constant of electron transfer between CO_2 and ester (○) and nitrile (▼) anion radicals with the standard free energy of the reaction (in DMF + 0.1 M *n*-Bu_4NCLO_4). Temperature 25 °C. For the definition of lines a and b, see the text.

Discussion

Figure 3 shows how the rate constant of the electron transfer reaction varies with the Figure 3 & standard free energy of the reaction ($\Delta G°$ (eV) = $E°_{cat} - E°_{CO_2}$ (V) with $E°_{CO_2} = -2.21$ V vs SCE) in the ester and nitrile series. Concerning the ester series, we note that on the right-hand side of the plot, log *k* varies with $\Delta G°$ by *ca.* 1/(120 mV) (line a) as expected for a simple electron transfer reaction in a driving force range around zero where the symmetry factor is close to 0.5. However, on the left-hand side, the average slope (line b) is closer to 1/(60 mV). The backward et reaction may be controlled jointly by activation and diffusion. Thus, the rate constant for the forward step would be expressed by eq 1 (k_D is the diffusion-limited

$$\frac{1}{k} = \frac{1}{k_{act}} + \frac{1}{Kk_D} \qquad (1)$$

bimolecular rate constant). Such mixed activation−diffusion-controlled kinetics have been observed previously in reactions of aromatic anion radicals with aryl halides[5b] and aryl methyl sulfides.[5d] A possible interpretation of the observed variation of *k* with $\Delta G°$ in Figure 3 could thus be that, in the high driving force zone (a), activation control predominates ($k = k_{act}$), whereas, in the low driving force zone (b), the reverse reaction is under diffusion control. Within this framework, line a in Figure 3 was drawn as the best fitting Marcus parabola (eq 2)

$$\log k = \log A - (F/RT)\Delta G_0^{\ddagger}(1 + \Delta G°/4\Delta G_0^{\ddagger})^2 \qquad (2)$$

through the right-hand side points with a preexponential factor $A = 3 \times 10^{11}$ M^{-1} s^{-1} and an intrinsic barrier free energy $\Delta G_0^{\ddagger} = 0.439$ eV.[5a] The latter value is qualitatively reasonable in view of solvent reorganization and of the change in geometry (from linear to bent[18]) attending electron transfer to the CO_2 molecule.

Under such conditions, it is also predicted that the linear extrapolation of the 1/(60 mV) line should reach $k = k_D$ for $K = 1$, i.e., for $\Delta G° = 0$, meaning that within this endergonic region the reverse reaction would be diffusion-controlled. As seen in Figure 3, the value of *k* for $\Delta G° = 0$ is only 1.8×10^5 M^{-1} s^{-1}, much smaller than the diffusion limit ($k_D = 10^{10}$ M^{-1}

s^{-1}). However, it may be conceived that the diffusion-controlled formation of the successor complex from the separated products would be slowed by an unfavorable work term. We will discuss this point starting from the scheme below (A and B represent the ester or nitrile molecules and their anion radicals, respectively, and P stands for CO_2 and Q for $CO_2^{\bullet-}$):

$$A + Q \underset{k_D^{-R}}{\overset{k_D^{R}}{\rightleftharpoons}} AQ \underset{k_{-e}}{\overset{k_e}{\rightleftharpoons}} BP \underset{k_D^{-P}}{\overset{k_D^{P}}{\rightleftharpoons}} B + P$$

According to the Debye−Smoluchowski model[19]

$$k_D{}^R = \frac{k_D}{d\int_d^\infty \exp\left[\frac{Fw_R(x)}{RT}\right]\frac{dx}{x^2}} \text{ with } k_D{}^{-R} = \frac{k_D{}^R}{K_R}$$

$$k_D{}^P = \frac{k_D}{d\int_d^\infty \exp\left[\frac{Fw_P(x)}{RT}\right]\frac{dx}{x^2}} \text{ with } k_D{}^{-P} = \frac{k_D{}^P}{K_P}$$

x is the distance between the centers of the (hard sphere) reactant or product molecules, and d is the closest approach value of x. $w_R(x)$ and $w_R(x)$ are the distance dependent work terms, and K_R and K_P are defined by

$$-\frac{RT}{F}\ln K_R = w_R(d) = w_R$$

$$-\frac{RT}{F}\ln K_P = w_P(d) = w_P$$

Since the nature of the interactions and of their variation with distance are not precisely known, we may consider that they are bracketed by the two limiting situations represented in the scheme below:

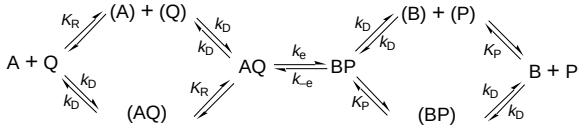

The lower pathways for the formation of the precursor and successor complexes correspond to short distance interactions (the interactions vanish within a distance much shorter than the size of the (mutual) diffusion layer). Then $k_D{}^R = k_D$ and $k_D{}^R = k_D$ for the reactants and $k_D{}^P = k_D$ and $k_D{}^{-P} = k_D/k_P$ for the products. In other words, an unfavorable work term accelerates the decomposition of the precursor and successor complexes into the separated reactants and products, respectively, while it leaves unchanged the rate of formation of the precursor and successor complexes from the separated reactants and products, respectively. Thus, the rate constant, k_+, for the endergonic conversion of A + Q into B + P is expressed as

$$k_+ = k_D\frac{K_RK_e}{K_P} = k_D\exp\left[-\frac{F}{RT}(E^\circ_{cat} - E^\circ_{CO_2})\right]$$

while $k- = k_D$. It thus appears that the experimental data in the endergonic region of Figure 3 cannot be accounted for by considering that the reverse reaction is under diffusion control even if the formation of the successor complex from the separated products involves an unfavorable work term.

The upper pathways for the formation of the precursor and successor complexes correspond to long distance interactions (the interactions remain the same over the whole (mutual) diffusion layer). This is the situation where the effect of unfavorable work terms on the formation of the precursor and successor complexes would be maximal. Then $k_D{}^R = K_Rk_D$ and $k_D{}^{-R} = k_D$ for the reactants and $k_D{}^P = K_Pk_D$ and $k_D{}^{-P} = k_D$ for the products. In other words, an unfavorable work term slows the decomposition of the precursor and successor complexes into the separated reactants and products, respectively, while it leaves unchanged the rate of formation of the precursor and successor complexes from the separated reactants and products, respectively. Thus, the rate constant, k_+, for the endergonic conversion of A + Q into B + P is expressed as

$$k_+ = k_DK_RK_e = k_DK_P\exp\left[-\frac{F}{RT}(E^\circ_{cat} - E^\circ_{CO_2})\right]$$

while $k_- = k_Dk_P$ (the rate constant for the reverse reaction is smaller than k_D if the work term for the formation of the successor complex from the separated products is unfavorable).

The interpretation of the 1/(60 mV) straight line in Figure 3 along those lines would thus imply a long-distance repulsive interaction worth *ca.* 0.3 eV between the ester molecule and $CO_2^{\bullet-}$. This is extremely unlikely; if any, the only interaction one could envision is a slight attractive interaction between the negative charge in $CO_2^{\bullet-}$ and the polarizable ester molecule.

These observations rule out the possibility that the 1/(60 mV) line in the small driving force region could be due to diffusion control of the reverse et reaction. This is a first indication that reaction et cannot be regarded as a simple outer-sphere electron transfer process.

Furthermore, it appears that there is no possibility to fit the whole set of data points with a single Marcus correlation line. Indeed, forced application of eq 2 for fitting all the points leads to obviously unrealistic values of A, 1.9×10^5 M^{-1} s^{-1}, and of $\Delta G_0^{\ddagger}$, 0.058 eV. The impossibility to interpolate the whole set of k values with a single Marcus parabola is a second indication that the reaction cannot be regarded as a simple outer-sphere process. These observations suggest that the reaction possesses an inner-sphere character or, equivalently, that it may be viewed as the transfer of an electron pair rather than of a single electron. In this framework, the results can be rationalized by a mechanism involving two successive steps as depicted in the following reaction scheme (or similar reactions in the nitrile case):

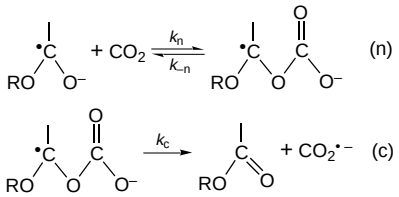

In the framework of such a mechanism, the overall rate constant k is related to the rate constants of each step according to eq 3.

$$k = \frac{k_nk_c}{k_{-n} + k_c} \quad (3)$$

Both the standard free energy and the activation barrier of reaction c should not depend much on the substituents on the phenyl ring. Indeed the effect of conjugation between the unpaired electron and the phenyl ring in the radical of the left-

(19) (a) von Smoluchowski, M. *Phys. Z.* **1916**, *17*, 557. (b) von Smoluchowski, M. *Phys. Z.* **1916**, *17*, 585. (c) von Smoluchowski, M. *Z. Phys. Chem.* **1917**, *92*, 129. (d) Debye, P. *Trans. Electrochem. Soc.* **1942**, *82*, 265. (e) Andrieux, C. P.; Savéant, J.-M. *J. Electroanal. Chem.* **1986**, *205*, 43.

hand side are likely to parallel the effect of conjugation between the carbonyl group and the phenyl ring in the right-hand side of the reaction. This is also likely to be true for the effect of R. The variation of K_n ($=k_n/k_{-n}$) in the series thus follows the variation of $E°_{cat}$. In the less negative end of the catalyst potentials, K_n is small, and therefore k_n is small and k_{-n} is large. Thus k_{-n} tends to become larger than k_c, and thus, $k = K_n k_c$. Under these conditions, log k varies by one unit when $E°_{cat}$ varies by 60 mV. When $E°_{cat}$ becomes more and more negative, K_n and k_n increase and k_{-n} decreases. A point will thus be reached where $k_{-n} < k_c$, meaning that forward reaction n becomes the rate-determining step. From there on log k is expected to vary by 1/(120 mV). These predictions fit the data obtained in the ester series.

The assumption that the standard free energy and the activation barrier of reaction c do not depend on the overall driving force for the generation of $CO_2^{\bullet-}$ might be too simplistic. In the framework of the above reaction scheme, a more general interpretation may be as follows. We assume that the standard free energies for reactions n and c are proportional to the standard free energy for the overall reaction:

$$\Delta G_n° = \gamma_n(E°_{cat} - E°_{CO_2}) \qquad \Delta G_c° = \gamma_c(E°_{cat} - E°_{CO_2})$$

Thus

$$\gamma_n + \gamma_c = 1 \tag{4}$$

It may also be assumed that the activation free energies of both reactions n and c are approximate linear functions of their respective standard free energies α_n and α_c as slopes. Thus, in the low driving force region

$$\frac{RT}{F}\ln k = \frac{RT}{F}\ln K_n k_c = \ln A_c + (\gamma_n + \alpha_c\gamma_c)(E°_{cat} - E°_{CO_2})$$

and in the high driving force region

$$\frac{RT}{F}\ln k = \frac{RT}{F}\ln k_n = \ln A_n + (\alpha_n\gamma_n)(E°_{cat} - E°_{CO_2})$$

From the experimental slopes of the log k vs $E°_{cat} - E°_{CO_2}$ plot (Figure 3), it follows that

$$\gamma_n + \alpha_c\gamma_c = 1 \tag{5}$$

and

$$\alpha_n\gamma_n = 0.5 \tag{6}$$

The four variables γ_n, γ_c, α_n, and α_c are thus related by eqs 4−6. Thus, in the framework of the two-step reaction scheme, γ_c and α_c are not necessarily equal to zero.

Whatever the exact value of these proportionality coefficients, the two-step reaction scheme offers a likely explanation of the observation that the reaction is not a simple outer-sphere process. The fact that the data points in the nitrile series fall above the ester correlation line lends further support to this conclusion.

Conclusions

Anion radicals of aromatic esters and nitriles are remarkably selective and fairly persistent homogeneous catalysts of the electrochemical reduction of carbon dioxide yielding exclusively oxalate. The generation of $CO_2^{\bullet-}$ by electron transfer from these donors is not a simple outer-sphere process, and therefore, catalysis is not strictly speaking of the outer-sphere type.[20] The reaction involves two successive steps. The first of these is an S_N2-type reaction where the oxygen or the nitrogen end of the anion radical catalyst binds to the carbon of CO_2. This reaction may equivalently be viewed as an inner-sphere process in which bond formation and electron transfer are concerted. The $CO_2^{\bullet-}$ anion radical is eventually produced after homolytic cleavage of the bond thus formed. Such a reaction mechanism bears a strong resemblance with what happens when aromatic anion radicals are reacted with alkyl halides, where, in the absence of steric hindrance, the most favorable pathway is also of the S_N2 type.[5b,c]

Experimental Section

Chemicals. DMF (Carlo Erba, RPE) was kept over anhydrous Na_2CO_3 for several days and stirred from time to time. It was then fractionally distilled under reduced pressure under N_2 twice and stored in a dark bottle under N_2. In order to remove as much residual water as possible, the solvent was repeatedly percolated before use through a column of neutral alumina (Merck, activity grade 1) previously activated overnight at 360 °C under vacuum. Tetra-*n*-butylammonium perchlorate (Fluka purum) was recrystallized twice from a 2:1 water−ethanol mixture and then dried in a vacuum oven at 60 °C. Carbon dioxide (99.998%) was supplied by SIAD (Italy). The solubility of the gas in DMF (0.199 M at 25 °C and 1 atm of pressure) at various temperatures and various partial pressures has been previously reported.[21] DMF solutions containing various concentrations of CO_2 were prepared by saturating the solvent with appropriate mixtures of CO_2 and argon. The apparatus used for the preparation of the gas mixtures and the method of calculating CO_2 concentrations in the solution from its partial pressure in the gas phase were previously described.[21]

The commercially available catalysts methyl 4-methylbenzoate, methyl 3-methylbenzoate, methyl 2-methylbenzoate, ethyl benzoate, phenyl benzoate, dibutyl phthalate, dimethyl phthalate, and dipropyl phthalate (from Aldrich Chemie), methyl benzoate (Janssen), benzonitrile (Fluka), 2-tolunitrile (Ega-Chemie), methyl 4-phenylbenzoate (Heraeus), diisobutyl phthalate (Carlo Erba), ethyl 3-fluorobenzoate (Sigma), and 4-cyanobiphenyl (K & K) were used as received. Phenyl 3-methylbenzoate and phenyl 4-methylbenzoate were prepared from 3-methyl- or 4-methylbenzoic acid and phenol, respectively, as previously described.[22] Methyl 3-phenoxybenzoate was prepared by refluxing 3-phenoxybenzoic acid in methanol in the presence of sulfuric acid.[23]

Electrochemical Instrumentation and Procedures. The *cyclic voltammetric* measurements were made with a PAR Model 173 potentiostat, a programmable function generator Amel Model 568 and a 2090 Nicolet oscilloscope. An Amel Model 863 *X*−*Y* recorder was used for recording the cyclic voltammograms. A mercury microelectrode was used as the working electrode and a platinum wire as the counterelectrode. The working electrode was made from a 2-mm-diameter platinum sphere coated with mercury after electrolytic deposition of silver. The reference electrode was Ag/AgI/*n*-Bu_4NI 0.1 M in DMF whose potential was always measured compared to the SCE, to which all potentials are finally referenced. Both the reference

(20) (a) There are two types of homogeneous catalysis of electrochemical reactions. In redox catalysis,[17,20b] the reduced form of the catalyst couple is merely an outer-sphere electron donor that shuttles electrons from the electrode to the substrate. This homogeneous electron transfer is subject to the same activation/ driving force limitations as the outer-sphere electron transfer at an inert electrode. The very existence of a catalytic effect thus derives from a physical rather than a chemical process, namely, the dispersion of the electrons in the same three-dimensional space as the substrate instead of the two-dimensional availability of the electrons at the electrode surface. In chemical catalysis, the interactions between the reduced form of the catalyst and the substrate are more intimate, involving the transient formation of an addition product between the reduced form of the catalyst and the substrate before regeneration of the oxidized form of the catalyst. (b) Andrieux, C. P.; Dumas-Bouchiat, J.-M.; Savéant, J.-M. *J. Electroanal. Chem.* **1978**, *87*, 39.

(21) Gennaro, A.; Isse, A. A.; Vianello, E. *J. Electroanal. Chem.* **1990**, *289*, 203.

(22) Hashimoto, S.; Furukawa, I. *Bull. Chem. Soc. Jpn.* **1981**, *54*, 2227.

(23) Ceccon, A.; Gentiloni, M.; Romanin, A.; Venzo, A. *J. Organomet. Chem.* **1977**, *127*, 315.

electrode and the counterelectrode were separated from the working electrode compartment by glass frits and salt bridges.

The diffusion coefficient of CO_2 in DMF has been previously found to be 2.7×10^{-5} cm^2 s^{-1}.[3d] For the catalyst we have found an average value of 0.8×10^{-5} cm^2 s^{-1}. These values were used in the construction of the working curves for extracting the rate constants from the cyclic voltammetric data.

Preparative scale experiments were performed in a gas-tight electrolysis cell under galvanostatic conditions with a current density of 1.6 mA/cm^2. Before the electrolysis was started, a solution saturated either with CO_2 alone or with a mixture of CO_2 and argon was prepared by bubbling the gas into the catholyte for about 30 min. During electrolysis, the cell was maintained in contact with a gas reservoir containing CO_2 at the appropriate partial pressure. A mercury pool of 12.4 cm^2 was used as the cathode. The same stirring rate was used in all the experiments in order to achieve reproducible hydrodynamic conditions.

Electrolysis products present in both the gas and liquid phases were analyzed by chromatographic techniques. Carbon monoxide and formic acid were analyzed on a Varian 3700 gas chromatograph equipped with a thermal conductivity detector, using helium as the carrier gas. CO was analyzed only in the gas phase using a molecular sieve column. Since the solubility of CO in dipolar aprotic solvents is very low,[24] the quantity of CO present in solution was considered to be negligible. Samples were extracted from the gas phase of the working electrode compartment with a gas syringe through a septum cap. To detect formate, the solution was first esterified by addition of methyl iodide to a portion of the electrolyzed solution.[25] The resulting solution in DMF was then analyzed by GC using a GP 10% SP-1200, 1% H_3PO_4 Supelco column. Oxalate was directly analyzed in HPLC with a Perkin-Elmer Series 4 liquid chromatograph equipped with a UV detector operating at 210 nm, using an Aminex HPX-87H ion exchange column eluted with 0.01 N H_2SO_4, on which conversion of oxalate to oxalic acid takes place. The validity of this procedure was checked by comparison with the classical permanganate colorimetric method.[26]

Possible side products resulting from carboxylation of the catalyst

$$ArCO_2R + CO_2 + 2e^- \rightarrow ArCOCO_2^- + RO^-$$

or from spontaneous decomposition of the anion radicals[27]

$$ArCO_2R^{\bullet -} \rightarrow ArCO_2^- + RO^{\bullet}$$

were investigated but could not be detected. It should be emphasized that any two-electron process destroying the catalyst, even totally, would consume only a small fraction of the total charge passed as compared to the catalytic reaction. Since less than 30% of the catalyst is lost in all cases, such side reactions contribute negligibly to the total amount of charge. The 10−20% that are lacking in the charge balance (Table 2) are thus more likely due to the diffusion of the small fraction of the oxalate formed toward the anodic compartment where it is immediately reoxidized into CO_2.

Supporting Information Available: A series of diagrams showing how the rate constant k was derived from the i_p/i_p° data by fitting with the appropriate theoretical working curves (computed by an implicit finite difference method) for each of the 14 ester and 3 nitrile catalysts (6 pages). See any current masthead page for ordering and Internet access instructions.

JA960605O

(24) (a) Wilhelm, B.; Battino, R. *Chem. Rev.* **1973**, *73*, 1. (b) Ercolani, C.; Moncelli, F.; Pennasi, G.; Rossi, G.; Antonini, E.; Acsenzi, P. *J. Chem. Soc., Dalton Trans.* **1981**, 1120.

(25) Wagenknecht, J. H.; Baizer, M. M.; Chruma, J. L. *Synth. Commun.* **1972**, 2, 215.

(26) Vogel, A. I. *Textbook of Quantitative Inorganic Analysis*, 2nd ed.; Longman, Green and Co.: London, 1955; p 275.

(27) (a) Seeber, R.; Magno, F.; Bontempelli, G.; Mazzochin, G. A. *J. Electroanal. Chem.* **1976**, *72*, 219. (b) Wagenknetch, J. H.; Goodin, R. D.; Kinlen, P. J.; Woodward, F. E. *J. Electrochem. Soc.* **1984**, *131*, 1559. (c) Masnovi, J. *J. Am. Chem. Soc.* **1989**, *111*, 9801. (d) Vincent, M. L.; Peters, D. G. *J. Electroanal. Chem.* **1992**, *327*, 121.